

## Oxide-Charge-Induced Localized States and Screening in a Model Two-Dimensional System

E. Glaser, R. Czaputa,<sup>(a)</sup> and B. D. McCombe

*Department of Physics and Astronomy, State University of New York at Buffalo, Buffalo, New York 14260*

G. M. Kramer

*Hughes Aircraft, Carlsbad, California 92008*

and

R. F. Wallis

*Physics Department, University of California, Irvine, California 92717*

(Received 21 April 1986)

Far-infrared measurements of intersubband absorption spectra of *n*-inversion layers in (100) Si metal-oxide-semiconductor field-effect transistors with mobile positive ions in the oxide have been carried out between 4.2 and 70 K. Results provide direct evidence for screening of localized states in this quasi two-dimensional electronic system as well as the existence of long band tails and impurity bands at low electron densities associated with subbands due to both the inequivalent conduction-band valleys.

PACS numbers: 73.20.Hb, 73.40.Qv, 78.50.Ge

The localization of charge carriers in quasi two-dimensional (2D) electronic systems has been a subject of considerable scientific interest recently. As shown by Hartstein and Fowler,<sup>1</sup> an excellent and unique tool for such investigations is provided by Si metal-oxide-semiconductor devices whose oxides are intentionally doped with positive ions that can be drifted controllably to the oxide-semiconductor interface when positive voltages are applied to the metal gate electrode. Because of the electrostatic confining potential in the Si at the Si-oxide interface, electron motion perpendicular to the interface is quantized into sets of subbands with the motion parallel to the interface unaffected. At low temperatures in thermodynamic and electrostatic equilibrium, electrons occupy only the lowest-lying subband in this system leading to 2D behavior as far as motion parallel to the interface is concerned. Above a threshold voltage the 2D electron density is linearly proportional to the applied (positive) gate voltage, and the electron density can be easily varied over approximately two orders of magnitude. The previous "dc" electrical transport studies provided initial evidence for localized states, band tails, and impurity bands in Na<sup>+</sup>-contaminated metal-oxide-semiconductor devices. More recent and more extensive experiments<sup>2</sup> support the interpretation of the low-temperature electrical transport data in terms of impurity bands over a range of positive oxide charge densities. However, recent studies of the frequency dependence of the dynamical conductivity<sup>3</sup> of similar structures coupled with theoretical calculations<sup>4</sup> have questioned the interpretation in terms of impurity bands.

The present far-infrared measurements provide direct evidence for the existence of impurity bands as well as for screening of these localized states in 2D

systems. In addition, studies as a function of temperature provide optical evidence for the existence of long band tails associated with the higher-lying set of subbands corresponding to conduction-band minima with a light effective mass for motion perpendicular to the interface.

Far-infrared absorption measurements were performed with the infrared electric field polarized perpendicular to the interface at 4.2 K and above on *n*-channel Si metal-oxide-semiconductor field-effect transistors (MOSFETs). The devices investigated were large (2.5×2.5 mm) thick-gate MOSFETs fabricated on 20-Ω cm *p*-type (100) Si substrates with mobile positive ions deposited in the oxide (sample 1, gate oxide thickness ~ 1400 Å) and with "clean" oxides (sample 2, gate oxide thickness ~ 2000 Å). Data were obtained with positive oxide charge density as a parameter, varied by the drifting at room temperature of controlled amounts of positive ions ( $\Delta N_{\text{ox}}$ ) to the SiO<sub>2</sub>-Si interface ( $0.8 \times 10^{11} \text{ cm}^{-2} \leq \Delta N_{\text{ox}} \leq 7.0 \times 10^{11} \text{ cm}^{-2}$ ) in the presence of positive gate voltages. Threshold voltages for various positive-ion drifts were determined by standard techniques at liquid nitrogen temperatures, and the value of the fixed oxide charge and the change with positive-ion drift were calculated from these results.<sup>5</sup> The residual positive interfacial oxide-charge number density ( $Q_{\text{ss}}$ ) was determined to be  $1.3 \times 10^{11} \text{ cm}^{-2}$  and is included in the total positive interfacial oxide-charge number density ( $N_{\text{ox}}$ ).

The far-infrared measurements were carried out in a light pipe system with a Fourier-transform interferometric spectrometer. The sample mounting arrangement, light coupling scheme, and gate modulation technique have been described previously.<sup>6</sup> The gate modulation spectrum is normalized to a background spectrum obtained with chopped light; the

resultant ratio spectrum is proportional to the absorption coefficient of the inversion layer at a given electron density.

Differential intersubband absorption spectra for sample 1 at a constant (low) inversion-layer electron density ( $n_s$ ) and several values of  $\Delta N_{ox}$  are shown in the inset to Fig. 1. The dominant line, observed at the lowest obtainable oxide charge density, shifts abruptly to higher frequencies above a minimum value of  $\Delta N_{ox}$  and broadens as the oxide charge is increased. Above  $\Delta N_{ox} = 4.0 \times 10^{11} \text{ cm}^{-2}$  the position of the shifted resonance peak is independent of interfacial oxide charge, up to and including the maximum drifted positive-ion density investigated.

A compilation of the transition-energy data as a function of  $n_s$  for several values of  $\Delta N_{ox}$  is shown in Fig. 1. At the lowest values of  $N_{ox}$  absorption lines are observed that, over the whole range of  $n_s$  investigated, agree in energy with calculated values<sup>7</sup> of the extended-state intersubband ( $0 \rightarrow 1$ ) transitions for the experimental depletion charge of  $1 \times 10^{11} \text{ cm}^{-2}$

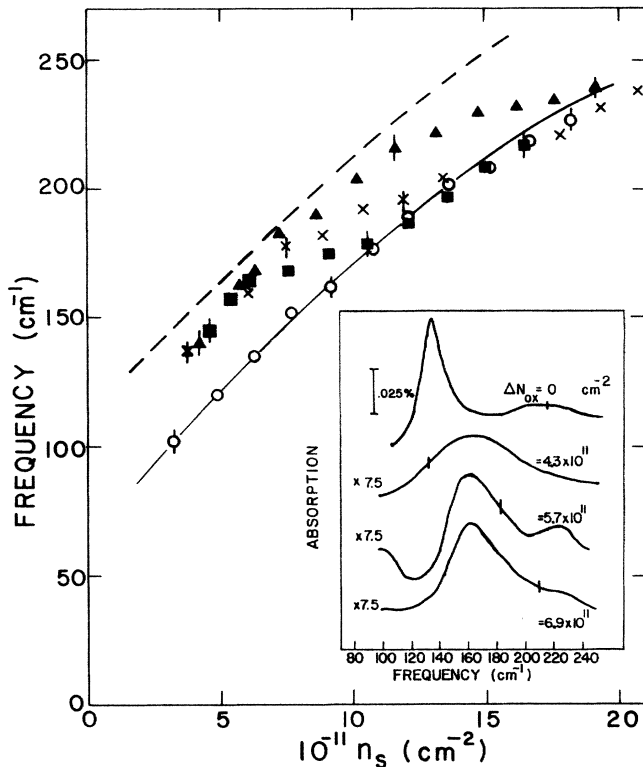


FIG. 1. Transition energy vs  $n_s$  at  $T = 4.2 \text{ K}$  for several values of  $\Delta N_{ox}$ : circles, 0; squares,  $4.3 \times 10^{11} \text{ cm}^{-2}$ ; crosses,  $5.7 \times 10^{11} \text{ cm}^{-2}$ ; and triangles,  $6.9 \times 10^{11} \text{ cm}^{-2}$ . Solid line, fit to the observed continuum transition energies. Dashed line, calculated impurity-derived intersubband transition energies vs  $n_s$  for the impurity ion  $11 \text{ \AA}$  into the  $\text{SiO}_2$ . Inset: Sub-band absorption spectra for several values of  $\Delta N_{ox}$  with  $n_s = (6.0 \pm 0.3) \times 10^{11} \text{ cm}^{-2}$ .  $N_{depl} = (1.0 \pm 0.15) \times 10^{11} \text{ cm}^{-2}$ . Bars indicate typical noise levels.

( $\pm 15\%$ ).

The limiting case of one electron bound to a single positive charge in the oxide has been studied extensively.<sup>8-10</sup> For realistic values of  $N_{ox}$  the impurities cannot be considered to be independent, and wavefunction overlap will result in an impurity band located below the quantized subband edge, or a tail of localized states for sufficiently disordered systems. In order to provide the simplest limiting-case basis for understanding the observed transition-energy results vs  $n_s$ , variational wave functions were utilized by Kramer and Wallis<sup>11</sup> to describe both continuum states and the states of an electron bound to an isolated charged impurity located at or near the  $\text{SiO}_2$ -Si interface in the presence of a constant electric field. The calculated  $0 \rightarrow 1$  continuum transitions in this model have been fitted (solid line) to the observed  $\Delta N_{ox} = 0$ ,  $0 \rightarrow 1$  transition energies in order to obtain the relationship between the effective constant electric field and the inversion layer density ( $F_{eff} - n_s$ ) for comparison with the experimental data.

Above a minimum value of  $N_{ox}$ , and over a range of  $n_s$  ( $n_s < N_{ox}$ ), the peaks of absorption lines are shifted to higher energy by about  $4 \text{ meV}$ , independent of  $\Delta N_{ox}$  between  $(4.3 \text{ and } 6.9) \times 10^{11} \text{ cm}^{-2}$ . Impurity-shifted intersubband transition energies have been obtained as functions of the surface electric field (with  $n_s$  vs  $F_{eff}$  determined from the  $\Delta N_{ox} = 0$  fit), with the distance of the impurity ion from the interface as a parameter.<sup>12</sup> With the positive ion  $11 \text{ \AA}$  away from the interface into the  $\text{SiO}_2$ , the dashed line plotted in Fig. 1 is obtained, consistent with present experimental results at low  $n_s$  as well as other experiments.<sup>13</sup> This model is clearly oversimplified, but the agreement with the experimental results for this range of  $\Delta N_{ox}$  lends support to an interpretation of the shifted lines in terms of transitions from an impurity band associated with the zeroth subband to an impurity band associated with the first excited subband.

Recently, experimentally observed shifts with oxide charge density of the subband resonance for  $n$  accumulation layers in similar structures has been interpreted<sup>3</sup> in terms of a self-energy shift, in a memory-function approach, due to increased scattering in the absence of an impurity band. For  $n_s = 3 \times 10^{11} \text{ cm}^{-2}$  this theory predicts a monotonically increasing shift ( $\sim 60\%$  for  $N_{ox}$  between  $4 \times 10^{11}$  and  $8 \times 10^{11} \text{ cm}^{-2}$ ) to higher energies with  $N_{ox}$  of the maximum of the frequency-dependent conductivity associated with the  $0 \rightarrow 1$  subband transition. We emphasize that the present experimentally observed shift is independent of  $\Delta N_{ox}$  over this range. In addition, for  $\Delta N_{ox} < (3-4) \times 10^{11} \text{ cm}^{-2}$  there is no observed shift of the subband absorption peak.

As  $n_s$  is increased beyond  $N_{ox}$ , the transition energies of the shifted lines approach the  $\Delta N_{ox} = 0$  sub-

band transition energies, and are coincident with this curve within experimental error for  $n_s$  greater than approximately  $2N_{ox}$  (see Fig. 1). In this region, it appears that there is strong screening of the positive ions by the excess mobile electrons in the inversion layer. The effective binding energy of electrons to the positive ions becomes very small,<sup>14</sup> resulting in essentially all impurities being ionized at 4.2 K. These data provide direct evidence of screening of localized states in quasi 2D systems. Thus the optical transitions at *high* enough inversion-layer densities can be described in terms of the usual subband transitions in the presence of a large density of screened Coulomb scattering centers.<sup>15</sup>

In order to investigate further the nature of the localized states and optical transitions in this system, the temperature dependence of the intersubband transitions was studied at low  $n_s$ . Initial temperature-dependent studies were carried out on sample 1 for  $\Delta N_{ox} = 0$ . As shown in the lower panel of Fig. 2, the peak energy of the  $0 \rightarrow 1$  intersubband resonance is essentially temperature independent over this range. This behavior is in qualitative agreement with a recent calculation<sup>16</sup> of the  $0 \rightarrow 1$  intersubband transition resonance for  $n$  inversion layers for the same temperature range and low values of  $n_s$  ( $< 10^{12} \text{ cm}^{-2}$ ). Near 20 K, a *second* peak becomes observable at energies above the  $0 \rightarrow 1$  transition; it shifts upward by 1.5 meV at  $T = 45$  K. This second peak is attributed to transitions ( $0' \rightarrow 1'$ ) originating in the ground subband states of the energetically higher-lying fourfold-degenerate conduction-band valleys, which become populated at elevated temperatures. The shift of this peak to higher frequencies at the higher temperatures is attributed to exchange lowering of the  $0'$  quasiparticle states as more electrons thermally occupy these states.<sup>17</sup> Calculations<sup>18</sup> of the ground ( $E_{0'}$ ) subband energy for the upper valleys for this range of  $n_s$  yield values close to the  $E_1$  subband energy for the lower valleys (15 to 20 meV) above the lowest-lying subband). Observation of intersubband transitions associated with the upper valleys at such low temperatures ( $k_B T \sim 2$  meV) is thus unexpected within an extended state model.

Temperature-dependent studies were also carried out on a "clean" oxide MOSFET with peak mobility  $\sim 15\,000 \text{ cm}^2/\text{V}\cdot\text{sec}$  (sample 2). In the upper panel of Fig. 2, representative differential absorption spectra are shown for this device. The relative intensities of the  $0 \rightarrow 1$  and  $0' \rightarrow 1'$  intersubband transitions for these two devices for similar values of  $n_s$  and temperature are *considerably* different. For  $n_s \sim 4 \times 10^{11} \text{ cm}^{-2}$ , the  $0' \rightarrow 1'$  intersubband resonance is the *dominant* transition for temperatures greater than 30 K in sample 1 while it remains weaker than  $0 \rightarrow 1$  in the clean sample (sample 2) up to the highest temperatures studied. Results from fitting the line intensities with

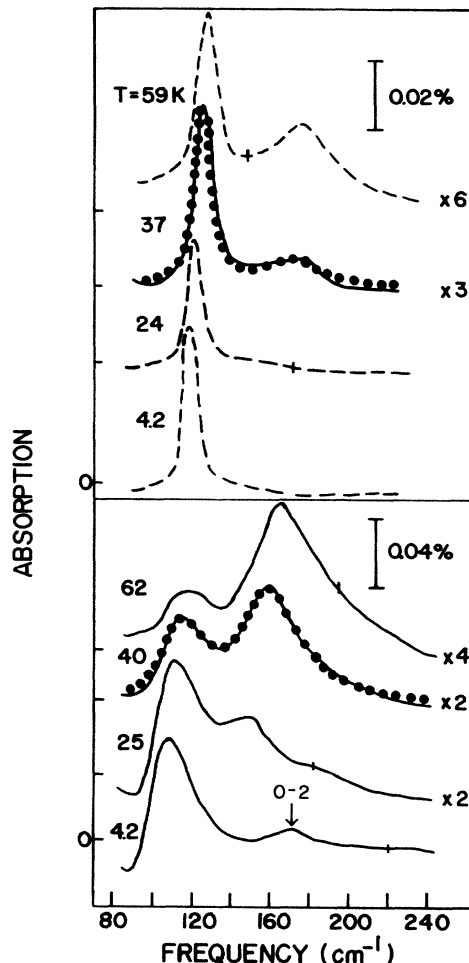


FIG. 2. (Lower) Subband spectra for sample 1 with  $\Delta N_{ox} = 0$  and  $n_s = 3.7 \times 10^{11} \text{ cm}^{-2}$ . (Upper) Subband spectra for sample 2 with  $n_s = 4.5 \times 10^{11} \text{ cm}^{-2}$ .  $N_{depl} = 1 \times 10^{11} \text{ cm}^{-2}$  for both devices. Traces are displaced vertically for clarity. Solid circles, Lorentzian oscillator fits described in text. Bars indicate typical noise levels.

Lorentzian oscillators are plotted as the solid circles in Fig. 2. From these fits the relative number densities of electrons in the various subbands are obtained for a fixed total electron density. A comparison of these relative occupancies with a three-subband, extended-state model and Fermi-Dirac statistics gives  $0-0'$  energy separations for the clean sample in good agreement with the theoretical calculations ( $\sim 14$  meV). On the other hand, similar fits for sample 1 with  $\Delta N_{ox} = 0$  yield *very small* apparent  $0-0'$  energy separations ( $\sim \frac{1}{3}$  of those predicted). From this comparison it is concluded that the small *apparent*  $0-0'$  separations obtained with an extended-state model are incorrect; and long band tails of localized states associated with the  $E_0$  and  $E_{0'}$  subbands greatly modify the density of states of the subbands for poorer quality samples.

In the presence of substantial mobile positive charge

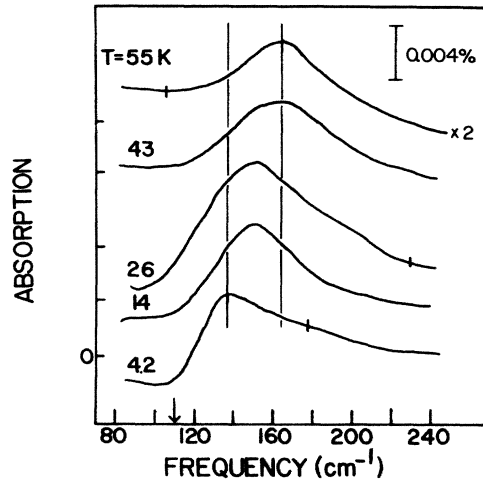


FIG. 3. Subband absorption spectra obtained for sample 1 with  $\Delta N_{\text{ox}} = 4.9 \times 10^{11} \text{ cm}^{-2}$  and  $n_s = 4.2 \times 10^{11} \text{ cm}^{-2}$ . Vertical lines indicate total shift. Arrow indicates position of the  $0 \rightarrow 1$  transition observed at  $T = 4.2 \text{ K}$  with  $\Delta N_{\text{ox}} = 0$ . Bars give typical noise levels.

these results are strongly modified. Representative differential absorption spectra for sample 1 for several temperatures with  $\Delta N_{\text{ox}} = 4.9 \times 10^{11} \text{ cm}^{-2}$  and  $n_s = 4.2 \times 10^{11} \text{ cm}^{-2}$  are shown in Fig. 3. For temperatures between 15 and 25 K the line broadens and the peak shifts to higher frequencies. The rapid shift of the peak is ascribed to increasing unresolved contributions to the overall line profile from impurity-subband transitions resulting from populating *bound states* (an impurity band) associated with the ground subband of the upper, fourfold-degenerate valleys. This shift is consistent with the results of a recent calculation<sup>19</sup> of the energy difference between impurity states of the lowest-lying two subbands associated with the upper valleys. Thus, the observation at elevated temperatures of impurity-derived transitions associated with the higher subband states from the higher-lying valleys for  $\Delta N_{\text{ox}} > 4 \times 10^{11} \text{ cm}^{-2}$  is consistent with the above model of localized states in long band tails extending well below the mobility edges, and the formation of impurity bands for *both* sets of valleys above a minimum value of added positive oxide charge density

( $\Delta N_{\text{ox}} \cong 3 - 4 \times 10^{11} \text{ cm}^{-2}$ ).

The support of the U. S. Office of Naval Research under Grant No. N0001483K0219 and the National Science Foundation under Grant No. DMR-8517634 is gratefully acknowledged. The authors are also indebted to A. Gold and F. Koch for helpful discussions.

(a) Present address: Institut für Experimental Physik, Karl Franzens Universität Graz, A-8010 Graz, Austria.

<sup>1</sup>A. Hartstein and A. B. Fowler, Phys. Rev. Lett. **34**, 1435 (1975).

<sup>2</sup>G. Timp, A. B. Fowler, and A. Hartstein, to be published.

<sup>3</sup>C. Mazure, F. Martelli, A. Gold, U. Grzesik, H. R. Chang, and F. Koch, Solid State Commun. **54**, 443 (1985); A. Gold, W. Gotze, C. Mazure, and F. Koch, Solid State Commun. **49**, 1085 (1984).

<sup>4</sup>A. Gold, Phys. Rev. B **32**, 4014 (1985).

<sup>5</sup>See, for example, S. M. Sze, *Physics of Semiconductor Devices* (Wiley, New York, 1981).

<sup>6</sup>B. D. McCombe, R. T. Holm, and D. E. Schafer, Solid State Commun. **32**, 603 (1979).

<sup>7</sup>T. Ando, Z. Phys. B **26**, 263 (1977).

<sup>8</sup>B. Vinter, Solid State Commun. **28**, 861 (1978).

<sup>9</sup>N. O. Lipari, J. Vac. Sci. Technol. **15**, 1412 (1978).

<sup>10</sup>B. G. Martin and R. F. Wallis, Phys. Rev. B **18**, 5644 (1978).

<sup>11</sup>See G. M. Kramer and R. F. Wallis, Surf. Sci. **113**, 148 (1982), and references therein.

<sup>12</sup>E. Glaser, R. Czaputa, B. D. McCombe, G. Kramer, and R. F. Wallis, in Proceedings of the Thirteenth Yamada Conference on Electronic Properties of Two-Dimensional Systems, Kyoto, Japan, 1985, Surf. Sci. (to be published).

<sup>13</sup>See, for example, D. J. DiMaria, J. Appl. Phys. **48**, 5149 (1977).

<sup>14</sup>B. Vinter, Phys. Rev. B **26**, 6808 (1982).

<sup>15</sup>E. Glaser, R. Czaputa, and B. D. McCombe, Solid State Commun. **54**, 715 (1985).

<sup>16</sup>S. DasSarma, R. K. Kalia, M. Nakayama, and J. J. Quinn, Phys. Rev. B **19**, 6397 (1979).

<sup>17</sup>S. DasSarma and B. Vinter, Phys. Rev. B **23**, 6832 (1981).

<sup>18</sup>B. Vinter, Phys. Rev. B **15**, 3947 (1977).

<sup>19</sup>G. M. Kramer and R. F. Wallis, Bull. Am. Phys. Soc. **31**, 396 (1986), and results to be published.